Non-hydrolytic sol-gel as a versatile route for the preparation of hybrid heterogeneous catalysts

Valentin Smeets,[1,*] Ales Styskalik,[2,*] Damien P. Debecker[1,*]

[1] Institute of Condensed Matter and Nanosciences - UCLouvain, 1348 Louvain-la-Neuve, Belgium

[2] Masaryk University, Department of Chemistry, Kotlarska 2, CZ-61137 Brno, Czech Republic

Corresponding authors: Damien Debecker (damien.debecker@uclouvain.be), Aleš Stýskalík (211138@mail.muni.cz), Valentin Smeets (valentin.smeets@uclouvain.be)

Abstract

The tools of sol-gel chemistry allow synthesizing a plethora of functional materials in a controlled bottom-up fashion. In the field of heterogeneous catalysis, scientists utilize sol-gel routes to design solids with tailored composition, texture, surface chemistry, morphology, etc. A field of investigations which shows great promises that of hybrid heterogeneous catalysts. Examples are flourishing to show that catalysts featuring a combination of inorganic and organic components often display improved activity, selectivity, or even chemical stability as compared to the purely inorganic counterparts. Yet, classic sol-gel methods face some well-known limitations – related to the different reactivity of the precursors and to the high surface tension of water – which complicate the tasks of chemists, specifically for the synthesis of hybrid catalyst. Non-hydrolytic sol-gel (NHSG) chemistry appears as a pertinent alternative. Being realized in the absence of water, NHSG routes allow reaching an excellent control over the solid composition, homogeneity, texture, and on the distribution of the organic and inorganic components at the nano- and microscales. In this review, we briefly recapitulate the main types of non-hydrolytic sol-gel routes and we present the modified protocols to hybrid materials. Then, we present an overview of the non-hydrolytic sol-gel approaches that have been proposed to synthesize hybrid heterogeneous catalysts. For both Class I and Class II hybrids, we discuss how the NHSG preparation has allowed tailoring the key properties that command catalytic performance. From this panorama, we argue that NHSG has a prominent role to play for the development of advanced hybrid heterogeneous catalysts.

Keywords

Nonhydrolytic sol-gel, organic-inorganic hybrid materials, heterogeneous catalysis, porous materials, metallosilicate

Declarations

Funding: This work was supported by the 'Communauté française de Belgique' through the ARC programme (15/20-069) and the European Union´s Horizon 2020 research and innovation programme under the Marie Skłodowska-Curie grant agreement No 751774.

Conflicts of interest/Competing interests: The authors have no conflicts of interest to declare that are relevant to the content of this article.

Code availability: Not applicable

Acknowledgements

Authors thank the 'Communauté française de Belgique' and the European Union´s Horizon 2020 research and innovation programme. D.P. Debecker thanks the Francqui Foundation for his "Francqui Research Professor" chair. V. Smeets is thankful to F.R.S.–F.N.R.S. for his FRIA PhD grant.

Graphical abstract

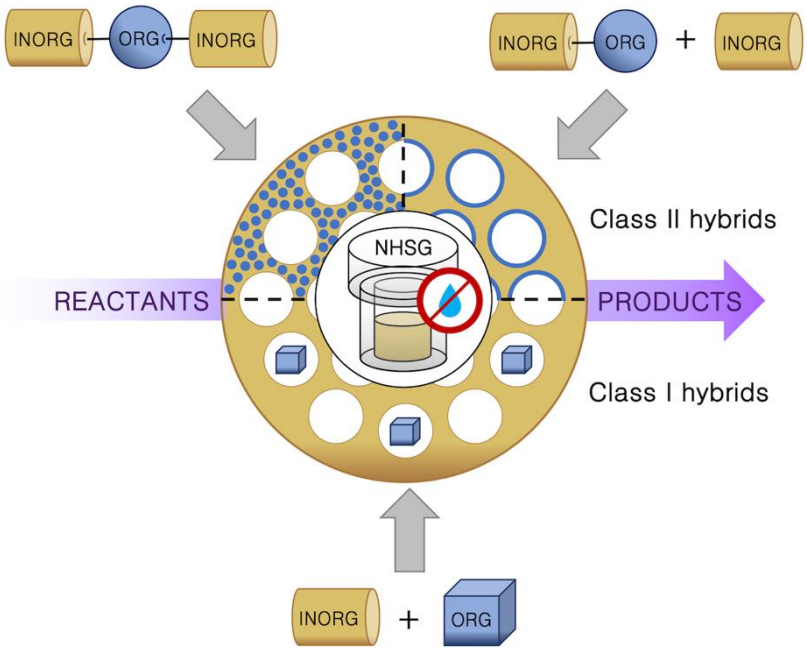

This review presents the non-hydrolytic sol-gel (NHSG) routes leading to organic-inorganic hybrid heterogeneous catalysts and shows how non aqueous synthesis conditions allow tailoring the key properties that command catalytic performance.

Highlights

- Sol-gel chemistry is an important synthesis toolbox for catalysis scientists
- Non-hydrolytic sol-gel is particularly useful for the synthesis of hybrid heterogeneous catalysts
- A brief summary of the principal non-hydrolytic sol-gel synthesis routes is presented
- A literature review of hybrid heterogeneous catalysts made by non-hydrolytic routes is proposed

1. Introduction

Historically, the development of innovative and efficient heterogeneous catalysts has triggered some of the most spectacular progress made in industrial chemistry [1]. Key catalyst discoveries have prompted advance in the production of commodities, specialty, fine chemicals, polymers, fuels, and also in the field of pollution control [2]. One can for example cite the discovery of Fe-based formulations catalyzing the synthesis of ammonia, Ni-based catalysts catalyzing hydrogenation reactions such as the methanation of CO_2 (Sabatier reaction), or acid catalysts triggering dehydration, alkylation or cracking reactions. In the petrochemical field, zeolites have played a major role [3]. At the end of the 20th century, the discovery of mesoporous molecular sieves expanded the field of applications in catalysis and beyond [4]. Nowadays, an important focus of catalysis science is on the development of heterogeneous catalysts that can help transition from a petro-based chemical industry to a bio-based one [5, 6]. In this context, catalysts are designed, not only to crack or modify or add chemical functionalities to existing hydrocarbon chains (as it is the case in petrochemistry), but rather to catalyze the removal of oxygen from the highly functionalized molecules that can be obtained from biomass (dehydration, hydrodeoxygenation, ketonization, decarboxylation, etc.). Moreover, the catalysts often have to operate in the presence of water, and therefore have to withstand hydrothermal conditions. Further expanding the library of heterogeneous catalysts available to tackle the challenges of the 21st century, we currently see a surge in the development of "hybrid catalysts".

Hybrid materials are constituted by organic components intimately mixed at the molecular or nanoscopic level with inorganic components, mainly metal oxides and derivatives; they have already found a wide range of applications [7, 8]. Hybrid materials are split into two main classes [9]. Class I hybrids represent materials where the organic and inorganic components additively exchange weak bonds (hydrogen, Van der Walls or ionic bonds). In Class II hybrids the organic and inorganic components are bonded through strong covalent or iono-covalent chemical bonds. Hybrid catalysts encompass a.o. surface-functionalized oxides [10], metal organic frameworks (MOF) [11, 12], periodic organosilicas (PMO) [13], supported organocatalysts [14], enzymes supported on inorganic carrier [15, 16], hybrid chemo-enzymatic heterogeneous catalysts (HCEHC) [17-19], metal complexes supported onto or encapsulated into inorganic carriers [20], and even encapsulated microorganisms [21]. As it will be discussed below, hybrid catalysts can feature several types of decisive advantages: immobilization of highly active and selective molecular catalytic species that can be easily recovered and reused, tuning of surface polarity to enhance catalyst stability against some specific deactivation mechanisms, carrying multiple types of active sites for cascade reactions, etc.

Using bottom-up synthesis methods, materials chemists are able to build, brick by brick, advanced catalytic materials featuring the desired active sites, surface functionalities, texture, and structure [22, 23]. Among those methods, sol-gel chemistry arguably represents one of the most versatile and powerful toolboxes for the preparation of tailored hybrid materials. In sol-gel chemistry, reactive molecular precursors in solution undergo controlled inorganic polycondensation reactions that lead to the formation of suspended oligomers which further reticulate to form a gel [24]. The latter can then be further processed by drying, calcination, etc. to form solid materials with the desired properties. Interestingly, the mild reaction conditions that are typically utilized in sol-gel chemistry allow envisaging the incorporation of organic components in oxides, to obtain Class I or Class II hybrids [25]. In the family of sol-gel chemistry routes, we argue that non-hydrolytic chemistry offers tremendous

possibilities, in particular for the preparation of heterogeneous catalysts and even more particularly for the preparation of tailored hybrid heterogeneous catalysts.

2. The principles of non-hydrolytic sol-gel for the preparation of hybrid materials

2.1. The working principles of non-hydrolytic sol-gel

Sol-gel chemistry is most often implemented in hydrolytic conditions. The precursors (metal or semi-metal alkoxides, halides, complexes (e.g. acetylacetonates), and other salts) are hydrolyzed by water to form reactive species which can then undergo inorganic polycondensation reactions. While the method is versatile, hydrolytic sol-gel faces two important limitations. First, hydrolysis and condensation rates can vary enormously among different precursors. Thus, if a mixture of precursors is to be used to prepare mixed oxides or hybrids, this kinetic mismatch can result in inhomogeneous materials. Second, the presence of water – which has a high surface tension – can be problematic for the preparation of highly porous materials: pores tend to shrink upon drying.

The central concept of non-hydrolytic sol-gel is to switch from classic hydrolytic conditions to non-aqueous conditions and to use oxygen donors other than water. A French group led by Corriu, Vioux, and Mutin extended pioneering reports [26-29] in this area and started back in the 1990s to study condensation reactions between metal chlorides and metal alkoxides resulting in metal oxides. In this case, the alkoxide was the oxygen donor; no water was used throughout the synthesis. The reaction rates leveled off, and highly homogeneous mixed metal oxides were obtained. Moreover, volatile organic solvents and products were easily removed, and thus product drying was streamlined. The resulting materials were intrinsically mesoporous and exhibited surface areas as high as 1000 $m^2 g^{-1}$. This research area has been coined "non-hydrolytic sol-gel," and many new routes to (mixed) metal oxides have been described with a strong focus on silicates [30-33]. In the following text, we first summarize the main NHSG reaction pathways with their respective oxygen donors (Section 2.2). Then, we highlight the modified versions of these protocols leading to hybrid materials (Section 2.3).

2.2. Summary of the main NHSG chemistry routes

Alkyl halide elimination is a reaction between a metal chloride and a metal alkoxide (Equation (1)). This condensation reaction leads to the formation of M−O−M bonds and, thus, inorganic oxides, while volatile alkyl chlorides are released as the reaction's volatile organic products. The metal alkoxide group can also be formed in situ by reaction of metal chloride with ether (Equation (2)), primary/secondary alcohols (Equation (3)), or to a lesser extent with dimethylsulfoxide (DMSO) [30-36].

$$\equiv M-Cl + R-O-M\equiv \longrightarrow \equiv M-O-M\equiv + RCl \quad (1)$$

$$\equiv M-Cl + ROR \longrightarrow \equiv M-O-R + RCl \quad (2)$$

$$\equiv M-Cl + ROH \longrightarrow \equiv M-O-R + HCl \quad (3)$$

Alternatively, tertiary alcohols and benzyl alcohol react with metal chlorides to give ≡M−OH groups and ^{t}alkyl- or benzyl chloride in a first step ((Equation (4), note the difference in comparison to the reaction between primary and secondary alcohol and metal chloride, Equation (3)). The subsequent condensation reaction then proceeds with the formation of inorganic oxide upon HCl release (Equation (5)). Thus, the overall balance of the reactions between metal chlorides and alcohols (primary, secondary, tertiary, and benzyl alcohol) is identical: products are inorganic oxide, HCl, and alkyl chloride. However, the benzyl alcohol route (Equations (4) and (5)) generally provides monodisperse

crystalline nanoparticles, while the application of primary and secondary alcohols (Equations 1−3) leads to amorphous and porous materials [37-43].

$$\equiv M{-}Cl + C_6H_5CH_2OH \rightarrow \equiv M{-}OH + C_6H_5CH_2Cl \quad (4)$$

$$\equiv M{-}OH + Cl{-}M\equiv \rightarrow \equiv M{-}O{-}M\equiv + HCl \quad (5)$$

Ester elimination (Equation (6)) is the reaction between metal alkoxides and acetates. It was studied in the 1950s by Bradley as a route to metal trimethylsilyloxides [44]. Later on, Caruso et al., used this route as a synthetic pathway to mixed metal oxo-clusters [45, 46] and oxides [47, 48]. Recently, it was discovered that acetoxysilanes condense with trimethylsilyl ester of phosphoric acid in a similar way providing highly homogeneous silicophosphates and acetic acid esters as organic products [49].

$$\equiv M{-}O{-}R + \equiv M{-}OC(O)R' \rightarrow \equiv M{-}O{-}M\equiv + RC(O)OR' \quad (6)$$

Another way to obtain highly porous and homogeneous metallosilicates was described recently as the acetamide elimination route. Reactions of acetoxysilanes with metal amides provide thoroughly condensed products based on M−O−M bonds and dialkylacetamide as a volatile organic product (Equation (7)) [50-55].

$$\equiv M{-}NR_2 + \equiv M{-}OC(O)R' \rightarrow \equiv M{-}O{-}M\equiv + R'C\,(O)NR_2 \quad (7)$$

Piers-Rubinsztajn reaction (or dehydrocarbon condensation) is the reaction between silanes and silicon alkoxides giving rise to Si−O−Si bonds and an alkane (Equation (8)). It is catalyzed by tris(pentafluorophenyl)borane and utilized mainly in the targeted synthesis of well-defined siloxane polymers [56-60].

$$\equiv M{-}H + R{-}O{-}M\equiv \rightarrow \equiv M{-}O{-}M\equiv + RH \quad (8)$$

Other recently described condensation pathway giving access to metal phosphates is based on the condensation between metal amides (particularly $Al(NMe_2)_3$) and trimethylsilylated phosphate (providing aluminophosphate materials upon silylamine elimination, Equation (9)) [61, 62].

$$\equiv M{-}NMe_2 + Me_3Si{-}O{-}P\equiv \rightarrow \equiv M{-}O{-}P\equiv + Me_2N{-}SiMe_3 \quad (9)$$

To the best of our knowledge, there are at least two NHSG routes that have not been used in the preparation of hybrid materials: (i) ether elimination and (ii) thermal decomposition of tris(^{t}butoxy)siloxydes [63-65]. This however does not mean that the preparation of organic-inorganic materials by these two methods would not be possible; the application of suitable precursors could, in principle, provide hybrid materials.

2.3. NHSG routes to hybrid materials

Class I hybrids formation in NHSG has been reported in several ways (Scheme 1): (i) the addition of a "spectator" species (e.g. organometallic species or metal complex) to the synthesis medium (a few examples are gathered in Scheme 1a); (ii) the addition of an organic polymer (e.g. surfactant) into the reaction mixture (Scheme 1b); (iii) the in situ formation of two interpenetrating polymer backbones (inorganic and organic, Scheme 1c). The first strategy typically results in the encapsulation of the organic species or complex into the inorganic matrix [66-76], whereas the second and third strategies mostly involve sacrificial pore-generating agents used to control the material texture (see below).

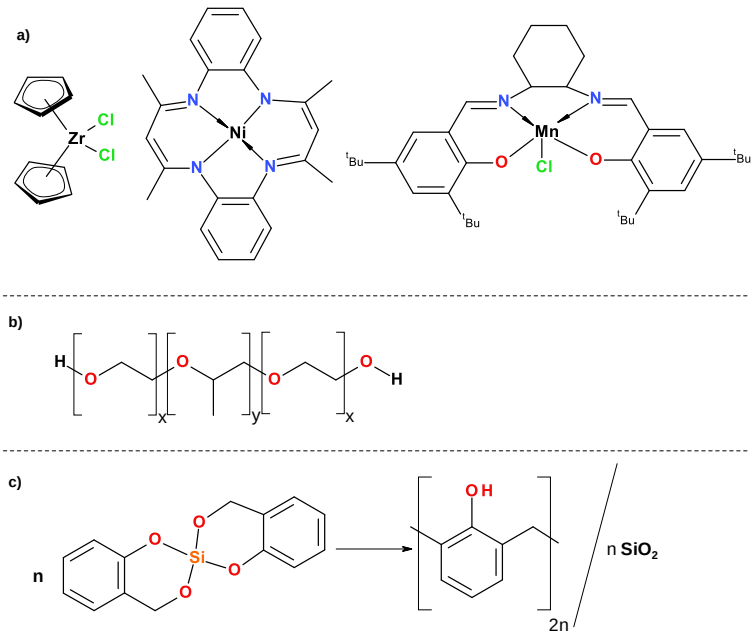

Scheme 1: Compounds used for preparation of Class I hybrids by NHSG: (a) organometallics and metal complexes, (b) pore generating agents, and (c) twin polymerization precursor and schematic mechanism of twin polymerization.

In this regard, the gels that are obtained by the NHSG routes described in Section 2.2 in the presence of an organic template (e.g. surfactant micelles) [50-53, 55, 77-79] must be considered as Class I hybrids. The most popular is the application of block copolymers based on polyethylene oxide and polypropylene oxide units as depicted in Scheme 1b, however other polymers (e.g. chitosan [78, 79]) were applied as well. Obviously, if such a hybrid material is further calcined to eliminate the sacrificial template and create pores in the final catalysts, the latter is no longer a hybrid.

A similar classification applies to materials prepared by the so-called twin polymerization developed by Spange et al. (Scheme 1c) [80-82]. This preparation route is based on the reaction of a well-defined metal-containing monomer leading to interpenetrating composite networks consisting of metal oxide and a polymer. These Class I hybrids are however usually transformed into purely inorganic materials by calcination, leading to high surface area (mixed) metal oxides and nanoparticles, such as SiO_2 [82], TiO_2 [81], SnO_2–SiO_2 [83], ZrO_2–HfO_2 [84], B_2O_3–SiO_2 [85], nitrogen-doped carbon (after SiO_2 removal by NaOH) [86], etc. Alternatively, Niederberger and co-workers obtained hybrid tungsten oxide-polybenzene monoliths by reacting tungsten(VI) isopropoxide with benzyl alcohol [87]. Rather than forming a suspension of crystalline tungsten oxide nanoparticles *via* the benzyl alcohol route (see Equations (4)-(5)), the isopropoxide ligand was exhanged with benzyl alcohol to form isopropanol and tungsten benzyl alcoholate which then condensed to form W–O–W bonds and dibenzyl ether (ether elimination route). The formed tungsten oxide nanoparticles then catalyzed the polymerization of the dibenzyl ether residues into polybenzene. The resulting monolithic material, which can be referred to as a Class I hybrid, was composed of the tungsten oxide nanoparticles embedded in the forming polymer.

Class II hybrids can obviously be prepared by post-synthetic grafting of purely inorganic oxides obtained via the NHSG pathways presented in Section 2.2 [88, 89]. It is noteworthy that the surface chemistry does not solely depend on Si–OH groups as in the case of hydrolytic sol-gel chemistry, but

on the contrary can be very rich (depending on the precursors and synthetic procedure used) and allow for targeted modification of selected sites [89].

Alternatively, the synthetic routes presented in Section 2.2 can be modified to incorporate "hybrid precursors" (Scheme 2) that will ensure the one-pot introduction of organic moieties into the network of the materials. In that case, the choice of the precursors will depend on the synthetic route applied and the organic groups attached.

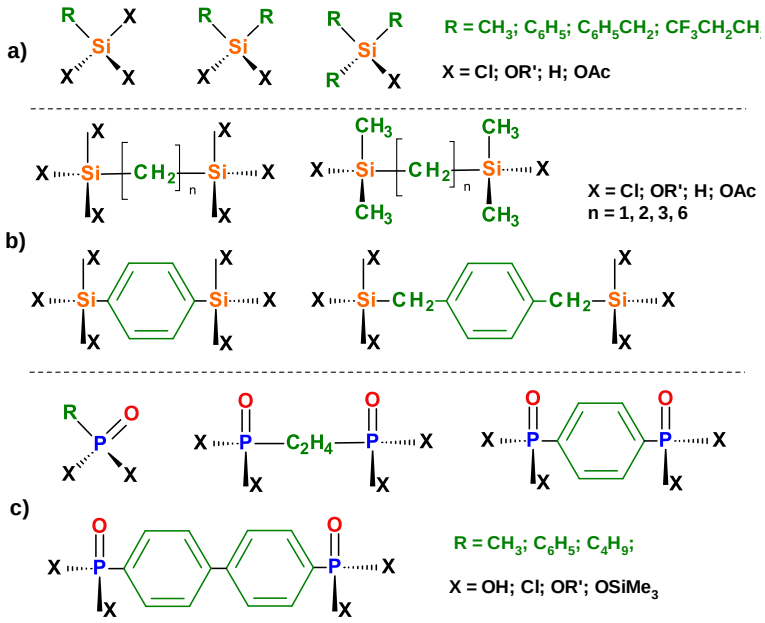

Scheme 2: Precursors applied for preparation of Class II hybrid materials via NHSG: (a) organosilanes with 1-3 terminal organic groups, (b) bis(silanes) bridged by various two-functional organic moieties, and (c) terminal and bridging phosphonate species.

In the case of alkyl halide elimination (Equation (1)), the incorporation of organic groups via stable Si–C bonds in commercially available alkyl-/aryl-chlorosilanes and alkyl-/aryl-alkoxysilanes is straightforward (Scheme 2a) [90-92]. Other strategies employing phosphonic acids and their derivatives (alkyl esters and chlorides) were also presented and led to hybrid metal phosphonates [93-97]. Similarly, organic groups were successfully embodied into the metal phosphonate materials via stable P–C bonds producing nanoparticles in the case of benzyl alcohol route (Scheme 2c, see also Equations (4)-(5)) [98, 99]. The benzyl alcohol route was also used to prepare ordered lamellar hybrid materials composed of crystalline rare earth oxide layers separated by intercalated organic benzonates or biphenolate moieties coordinated to the rare earth atoms *via* carboxylate functional groups [100].

NHSG routes that depend on the use of acetoxysilanes (i.e. ester elimination and acetamide elimination, Equations (6)-(7)) were shown feasible for hybrid materials preparation: alkyl-/aryl-acetoxysilanes were applied as hybrid precursors. Bridging organic groups increased network connectivity and were ideal for high surface area materials attainment (Scheme 2b) [50, 89, 101]. Moreover, hybrid silicophosphate materials prepared by ester elimination featured not only organic groups bound to Si atoms via Si–C bonds but also organic groups attached to P via P–C bonds [101]. These were introduced via trimethylsilylated phosphonates equipped with both terminal and bridging organic groups. The same family of precursors was used in trimethylsilylamine elimination and produced hybrid porous aluminum phosphonates (Scheme 2c, see also Equation (9)) [61].

The preparation of hybrid materials is inherent in Piers-Rubinsztajn condensation reaction (Equation (8)). Indeed, the theoretically possible synthesis of fully inorganic material would require the application of unstable SiH_4 as a precursor. On the contrary, the alkyl- and arylsilanes (Scheme 2a) show higher stability and are therefore applied in Piers-Rubinsztajn (dehydrocarbon condensation) reactions providing well-defined siloxane polymers. Recently, the condensation between diphenylsilane and trimethylborate was presented and led to a hybrid borosiloxane resin formation [60]. The hybrid material was based on $-(Si(Ph)_2-O-B)-$ moieties, and methane was released upon condensation.

A dedicated NHSG pathway can be implemented specifically to synthesize Class II hybrids. The possibility of reacting inorganic and organic precursors together was reported by Kejik et al. [102] The reaction between acetoxysilanes and polyfunctional phenols provides highly porous organosilicates, while acetic acid is eliminated as a condensation product (Equation (10)).

$$\equiv Si-OC(O)R' + HO-R_{aromatic}\equiv \rightarrow \equiv Si-O-R_{aromatic}\equiv + R'COOH \qquad (10)$$

Notably, such general ease of organic moieties embodiment via a one-step process is possible in NHSG due to the application of organic solvents and to the slowing down and leveling of the reaction rates during co-condensation (not only precursors containing different metals, but also with different types, sizes, and amounts of organic groups react at similar rates). The reaction rates can be slowed down to a point where targeted syntheses of organosilane building blocks become possible (Scheme 3) [34, 35, 57, 103-107]. These building blocks can be consequently condensed in a controlled fashion [105, 108-114], providing targeted nanostructured materials (e.g. well-defined siloxane structures or silica based hybrids with single catalytic sites).

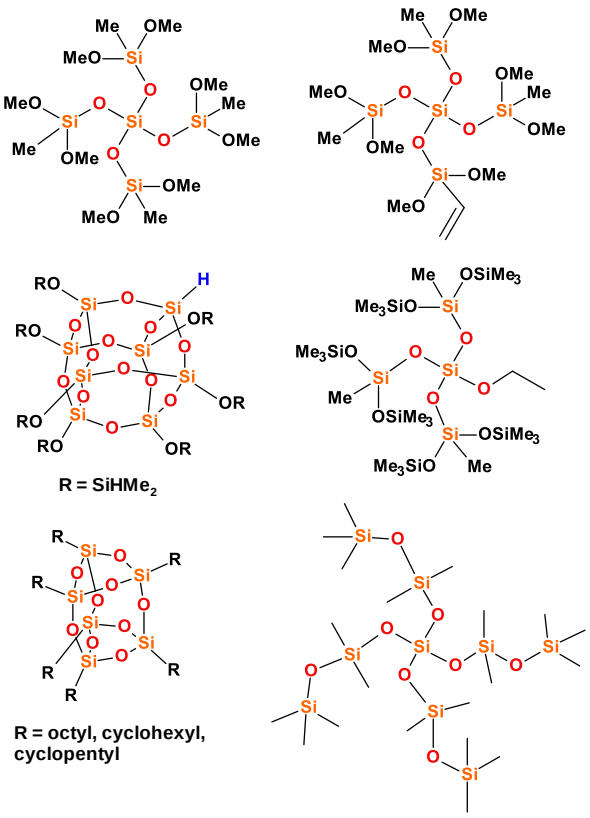

Scheme 3: Examples of molecular building blocks prepared by targeted non-hydrolytic condensation reactions.

Finally, it is noteworthy that the post-synthetic processing of the hybrid gel (for both Class I and II hybrids) might be markedly different from purely inorganic materials due to the necessity of organic groups preservation. This is true for both NHSG and classic (i.e. hydrolytic) sol-gel preparation routes. The volatile organic products of the condensation reactions as well as the unreacted organic groups can be removed via drying, (reactive) washing, vacuum annealing, or mild calcination (annealing). The maximum temperatures used in these processes must be carefully chosen to prevent the degradation of on-purpose incorporated organic groups. As such, hybrid heterogeneous catalysts may often show lower thermal stability as compared to purely inorganic counterparts, and this should be taken into account during catalyst preparation and operation. A stark organic groups thermal stability dependence on operating conditions (temperature, atmosphere, etc.) has been shown recently in the case of phenylene bridges in silsequioxanes: while it is known that these groups are stable up to 550 °C in dry air, this thermal stability limit dropped down to 400 °C upon introduction of 6.25 mol% of Al or Nb (based on Si). Moreover, the Si−C bond's hydrolysis was observed at a temperature as low as 205 °C when the metal-doped silsesquioxane materials were exposed to the moist atmosphere [115].

3. NHSG-made hybrid heterogeneous catalysts: review of the literature

Many NHSG-made inorganic catalysts have been reported in the literature, often showing enhanced performance in a wide range of catalytic applications, such as for example olefin metathesis [116-118], alkene epoxidation [51, 54, 119], oxidation of sulfur compounds [120], dehydration of bio-alcohols [55], transformation of ethanol to 1,3-butadiene [121], total oxidation of volatile organic compounds [122], aminolysis and alcoholysis of epoxides [50, 52, 53], α-methylstyrene dimerization [77], reduction of nitrogen oxides by hydrocarbons (HC-SCR) [123, 124], methane dry reforming [78], hydrodeoxygenation of model lignin monomers [118]. As stated above, the conditions of NHSG synthesis allow expanding the list to hybrid catalysts, and this field is currently emerging as a new land of opportunities. Table 1 and 2 gather the examples of hybrid heterogeneous catalysts prepared by NHSG discussed in this account (Class I and II, respectively).

3.1. Encapsulation of organometallics and metal complexes (Class I hybrids)

Class I hybrid heterogeneous catalysts prepared by non-hydrolytic sol-gel refer to the encapsulation of organometallics and metal complexes inside inorganic xerogels (Table 1). In such approach, the heterogeneization of the organic component is performed whilst the support is synthesized (see one example in Figure 1a).

Table 1: Survey of the literature for NHSG-made Class I hybrid heterogeneous catalysts.

Type of hybrid catalyst	Organic component [a]	Inorganic component	Targeted catalytic reaction	Observation	Reference
Encapsulation of metallocenes in SiO_2 and metalosilicates	Cp_2ZrCl_2, $(^nBuCp)_2ZrCl_2$, $(^iBuCp)_2ZrCl_2$, $(^tBuCp)_2ZrCl_2$, Cp_2TiCl_2, Cp_2HfCl_2, $EtInd_2ZrCl_2$, $Et(IndH_4)_2ZrCl_2$	SiO_2	Ethylene polymerization	Metallocene retained in the solid despite the absence of covalent bonds	[70, 76, 125]
	Cp_2ZrCl_2	SiO_2–MO_x (MO_x = TiO_2, CrO_3, MoO_3, WO_3)		Charge balance on Zr influenced by physico-chemical properties of the (hybrid) xerogels	[66, 68, 69]
		R-SiO_2 [b]		Tuneabe polymer properties	[67]
		Dual-shell SiO_2 structures		Positive impact on diffusion and protection of active sites against deactivation	[71, 126]
Encapsulation of metal complexes in Al_2O_3	Fe(III) and Mn(III) porphyrin	Al_2O_3	Oxidation of cyclooctene, styrene and cyclohexane Baeyer-Villiger oxidation of cyclohexanone	Enhanced active site accessibility Resistance against leaching, chemical degradation, and/or dimerization	[73, 75]
	Mn(salen) (Jacobsen catalyst)		Epoxidation of cyclooctene		[74]
	Ni(II) tetraazacomplex				[72]

[a] For conciseness, this column showing the part of the hybrid that contains the organic moieties is called "organic component" even though the organic moieties are actually brought by metal complexes or organometallic species.

[b] In these particular cases, the metal complex is encapsulated in a Class II hybrid material (R = methyl-, octyl-, octadecyl-, vinyl-, phenyl-, chloropropyl-, iodopropyl-, glycidoxypropyl-). Yet, since the catalytically active species is the metallocene complex - which is not chemically bound to the oxide surface but just entrapped - we propose to discuss them together with Class I hybrid catalysts.

Dos Santos and co-workers showed that metallocene complexes (Table 1, see also Scheme 1a) – which are used as catalysts for ethylene polymerization – can be advantageously encapsulated in silica-based matrices prepared by NHSG alkyl halide elimination route by simply adding the metallocene to the gel precursor solution (Figure 1a) [76]. The latter is typically composed of $SiCl_4$, tetraethyl orthosilicate (TEOS) and a small amount of $FeCl_3$ (catalyst of the sol-gel reactions). The gelation is carried out under

argon at 70°C to avoid the thermal degradation of the metallocene, and the resulting gel is successively washed and dried under vacuum [70]. The final metallocene content in such hybrids varied from 0.27 wt.% [70] to 3.54 wt.% [67].

Classic (hydrolytic) sol-gel routes are generally not compatible with the immobilization of metallocene catalysts due to the chemical lability of the complex. For example, in the case of bis(cyclopentadienyl) zirconium dichloride (Cp_2ZrCl_2), a large number of Zr-bidentate species – in which the labile ligand Cl is absent – are formed when entrapped in SiO_2 prepared through hydrolytic sol-gel processes because the latter features a high surface density of Si-OH groups [127]. The absence of the labile Cl ligand prevents the formation of the active polymerization centers, which are generated through alkylation of the complex in a reaction with methylaluminoxane (MAO) used as co-catalyst. A possible solution to this issue is to remove the -OH groups from the silica surface by applying a thermal treatment at high temperature (e.g. 723 K) [127]. More advantageously, the metallocene can be directly encapsulated through NHSG (Figure 1a). Effective one-step immobilization was demonstrated at mild temperatures without compromising the chemical structure of the complex and thus its catalytic properties [68, 70]. DR UV-visibile spectroscopy provided evidence of the integrity of Cp_2ZrCl_2 and Cp_2TiCl_2 chemical structures inside hybrids by identifying bands which could be assigned to ligand metal charge transfers (LMCT) Cl→M and Cp→M (M = Zr, Ti) [76, 125].

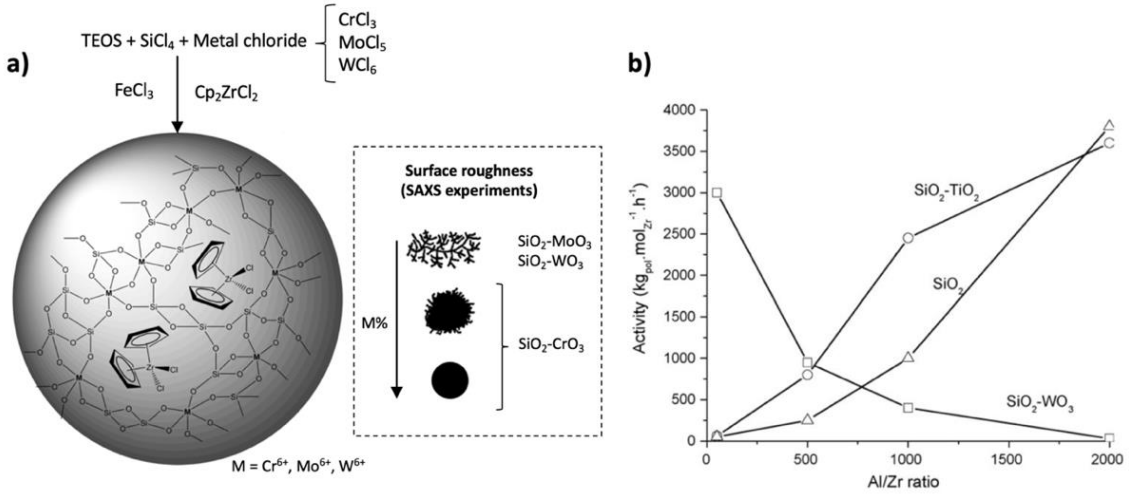

Figure 1: a) Schematic illustration of the immobilization of Cp_2ZrCl_2 in mixed oxides synthesized by NHSG. b) Catalytic activity of Cp_2ZrCl_2 encaspulated in SiO_2, SiO_2–TiO_2 and SiO_2–WO_3 as a function of the Al/Zr ratio. Adapted with permission from [66] and [69].

The porosity of the xerogels prepared by the alkyl halide elimination route favors interactions between the metallocene and the oxide surface [69]. In some cases, these interactions may change the electronic properties of the Zr center and thus affect the catalytic properties of the metallocene complex. Fisch *et al.* reported that the insertion of W or Ti in SiO_2 (*via* the addition of WCl_6 or $TiCl_4$ to the gel precursor solution) stabilized the encapsulated Cp_2ZrCl_2 complex through interactions with Lewis acid sites. This resulted in a reduction of the electron density on Zr as compared to the homogeneous complex [68, 69]. Such change in the electronic structure allowed the polymerization to occur at low concentrations of co-catalyst (expressed in terms of Al/Zr ratio, see Figure 1b) as compared to Cp_2ZrCl_2 encapsulated in SiO_2 [69]. Such reduction of the amount of co-catalyst is beneficial to the ethylene polymerization process as it may cut down the costs and generate lower amounts of aluminum residues in the polymer material [67].

Later on, Bernardes *et al.* extended the study of binary oxides as supports for Cp_2ZrCl_2 to SiO_2–CrO_3 and SiO_2–MoO_3 (Figure 1a) [66]. Interestingly, the authors found out that the reduction of the electron density on the Zr centers was not the only factor that governed the catalytic performance. SAXS experiments revealed that the size of the primary particles composing the xerogel and their degree of aggregation – which determine pore formation and surface roughness – was affected by the nature of the metal as well as by the metal content (see Figure 1a). The increase of the surface roughness could be correlated with an increase of the catalytic activity, suggesting that the active sites were more accessible in the gels having less condensed structures (SiO_2–MoO_3 and SiO_2–WO_3), whereas denser structures (SiO_2–CrO_3) hindered the access of monomers to the active sites. Based on a deconvolution of the polyethylene (PE) molar mass distributions, four distinct types of active sites could be identified in the hybrid catalysts, whereas there was only one in homogeneous Cp_2ZrCl_2. These additional sites produced PE with higher average molar mass compared to homogeneous Cp_2ZrCl_2, as a result of the internal morphology of the solid catalyst that hindered the occurrence of chain termination reactions. Based on these results, the authors suggested that PE properties could be advantageously tuned by changing the solid structure, *e.g.* by modifying the nature of the metal and/or the metal loading.

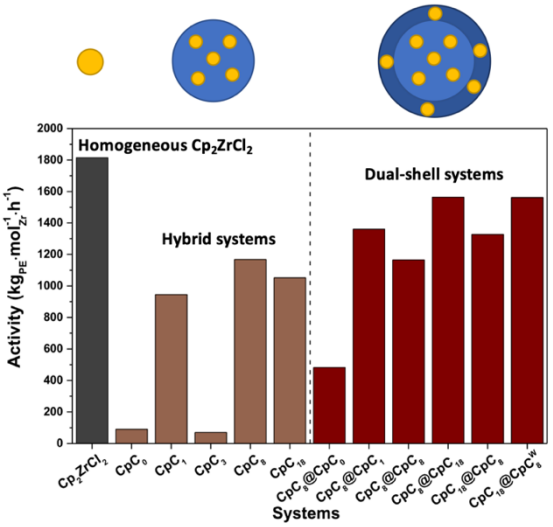

Figure 2: Activity in PE formation (Al/Zr = 500) of Cp_2ZrCl_2 ("Cp") encapsulated in Class II hybrid silica modified with various organic groups ("CpC_n", with C_0 = TEOS only, C_1 = methyltriethoxysilane, C_8 = octyltriethoxysilane, C_{18} = octadecyltrimethoxysilane) (brow) or in dual-layered silica structures ("$Cp_n@Cp_m^{(w)}$", with "Cp_n" the 1st layer and "$Cp_m^{(w)}$" the 2nd layer, possibly modified with W Lewis acid sites "w"). Adapted with permission from reference [71].

Cp_2ZrCl_2 was also encapsulated inside Class II hybrid silica xerogels obtained by NHSG alkyl halide elimination route [67]. In that case, SiO_2 was modified in one-pot using various organosilanes (footnote of Table 1) directly introduced in the gel precursor solution using a organosilane/$SiCl_4$/TEOS molar ratio of 1:3.3:1.7 (R-SiO_x/SiO_2 = 0.2). The presence of the organic moieties in these hybrid systems affected the interactions between the complex and the support, once again affecting the charge balance on Zr in a way that promoted PE formation (Figure 2). The introduction of the organic groups led to the suppression of the active sites responsible for generating long polymeric chains. The polymers produced with the complex encapsulated in hybrid silica were thus characterized by lower average molar mass compared to the polymers obtained with the complex encapsulated in plain silica. Very recently, the same authors managed to improve the activity and in-operation stability of Cp_2ZrCl_2 encapsulated in Class II hybrid silica by forming dual-layered structures *via* an iterative sol-gel process

which was claimed to enhance transport properties and protect active sites against degradation and poisonning (see Figure 2) [71, 126].

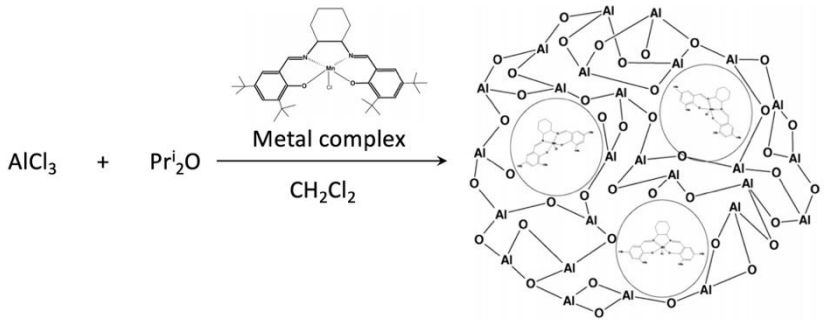

Figure 3: Schematic illustration of the preparation by the non-hydrolytic ether route of metal complex-Al_2O_3 hybrid catalysts, here illustrated for the encapsulation of the Jacobsen catalyst (Mn(salen)). Adapted with permission from reference [74].

Ciuffi and co-workers proposed to exploit NHSG routes (using various ethers or alcohols as oxygen donors) in order to encapsulate metal complexes used as oxidation catalysts (Fe(III) and Mn(III) porphyrins [73, 75], Mn(salen) [74], Ni(II) tetraazacomplex [72], Scheme 1a, see also Table 1) in amorphous alumina (see one illustration for Mn(salen) complex in Figure 3). In 2019, they reported the immobilization of iron(III) [5,10,15,20-tetrakis(2,6-dichloro-3-aminophenyl)-porphyrin] complex (abbreviated FeP) on Al_2O_3 prepared by the alkyl halide elimination route [75]. First, FeP and $AlCl_3$ were solubilized in diethyl ether (ether route, Equation (2)), or alternatively in dry ethanol (alcohol route, Equation (3)), which had the dual function of oxygen donor and solvent. This solution was refluxed for 4h at 110°C (under argon) and the resulting gel was further aged for 24h at room temperature in the reaction medium. The final hybrid xerogel ($Al_{alcohol}$-FeP or Al_{ether}-FeP) was obtained after extensive washing with EtOH/water mixture and drying at 100°C. The experimental loading of ironporphyrin complex in $Al_{alcohol}$-FeP was of 9.62 mg per gram of alumina.

The authors showed that changing the oxygen donor could result in a modification of the solid morphology as well as of its textural properties (S_{BET} of 309 $m^2\ g^{-1}$ and 100 $m^2\ g^{-1}$ for Al_2O_3 prepared by the alcohol and ether routes, respectively). Also, the distribution of the organic component in the solid changed as a function of the oxygen donor. Indeed, the alcohol route generated more hydroxyl groups at the surface, corresponding to a higher concentration of Brønsted acidic sites and a higher surface hydrophilicity. Thus, in the case of $Al_{alcohol}$-FeP, the complex was located preferentially on the surface. According to pyridine adsorption and thermagravimetric analysis, the amount of Brønsted acid sites as well as the hydrophilic character of the solids were reversed when FeP was inserted in alumina, with Al_{ether}-FeP being more hydrophilic than $Al_{alcohol}$-FeP.

The catalytic performance of the homogeneous FeP complex and of the heterogeneous Al-FeP catalysts were evaluated in the oxidation of cyclooctene, the oxidation of cyclohexene, and the Bayer-Villiger oxidation of cyclohexanone. Al_{ether}-FeP exhibited lower conversions than $Al_{alcohol}$-FeP for the oxidation of cyclooctene with iodosylbenzene as oxidant which was rationalized by the fact that the complex is readily available at the surface of the later catalyst. Further, no product was formed at all when using Al_{ether}-FeP as catalyst in the presence of anhydrous hydrogen peroxide. The authors attributed the absence of activity of Al_{ether}-FeP with H_2O_2 to the higher acidity of the hybrid catalyst that deactivated hydrogen peroxide when the latter was used as oxidant. Generally speaking, the

heterogeneous $Al_{alcohol}$-FeP catalyst showed higher conversions in the tested reactions compared to the homogeneous complex. The authors suggested that the FeP complex in its immobilized form was less hindered than in the homogeneous phase (low solubility of FeP in the solvent), which made the active sites more accessible to the reactants and contributed to increase the activity. In parallel studies, encapsulated FeP, Mn(salen) and Ni(II) tetraazacomplex also exhibited a higher chemical stability as the presence of the support avoided the chemical degradation of the complexes under catalytic conditions and/or prevented the formation of less active dimeric complexes [72-74].

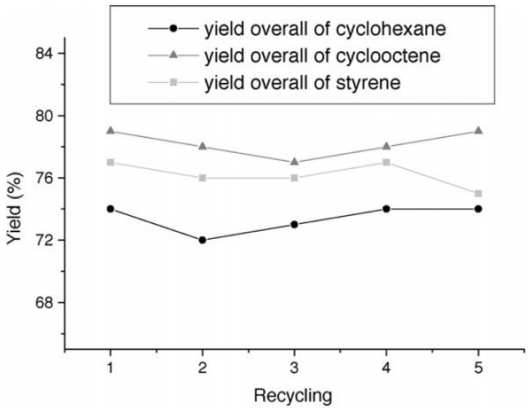

Figure 4: Recycling of the Mn(salen)-Al_2O_3 catalyst prepared by NHSG in the oxidation of cyclohexane, cyclooctene and styrene with 3-chloroperoxybenzoic acid (m-CPBA) as oxidant. Reproduced with permission from [74].

Owing to the stable interactions between the FeP complex and the support, the $Al_{alcohol}$-FeP catalyst could be reused three times in the oxidation of cyclooctene with anhydrous H_2O_2 without showing any sign of deactivation or metal leaching. The same behavior was observed for Jacobsen catalyst immobilized on Al_2O_3 by NHSG (Figure 4) [74]. On the opposite, similar hybrid catalysts prepared under hydrolytic conditions or by simple adsorption of the metal complex were prompt to complete metal leaching under reaction conditions [72, 73], which highlights the importance of NHSG in the preparation of this type of hybrid materials.

3.2. Organic functional groups incorporated through covalent bonds (Class II hybrids)

Class II hybrid catalysts prepared by NHSG refer to oxides and mixed oxides that are functionalized by pendant or bridging organic moieties which are bonded to the inorganic part of the material through strong (covalent) bonds.

One of the first example of application of hybrid materials prepared by NHSG and exploited in heterogeneous catalysis was probably the one reported by Lorret et al. [90] Silica-titania hybrid materials with Si:Ti ratio of 10 containing $MeSiO_3$ or Me_3SiO groups were prepared by a co-synthetic approach via alkyl halide elimination. It is noteworthy that the organic (terminal) groups loadings were very high (10−60 mol% based on Si) and still the materials were highly porous (930−1060 $m^2\ g^{-1}$; 0.72−1.28 $cm^3\ g^{-1}$, Figure 5). The synthetic procedure was very simple: one-pot NHSG synthesis followed by conventional drying. Neither template nor supercritical drying was necessary to produce these mesoporous materials. Hybrid titanosilicates were used as catalysts for epoxidation of cyclohexene oxide; their activity was comparable to hybrid silica-titania aerogels (dried under supercritical conditions) [90].

Table 2: Survey of the literature for NHSG-made Class II hybrid heterogeneous catalysts.

Type of hybrid catalyst	Organic component[a]	Inorganic component	Targeted catalytic reaction	Observation	Reference
Mesoporous hybrid titania-silica xerogels	CH_3Si, $(CH_3)_3Si$	TiO_2–SiO_2	Cyclohexene epoxidation	Very high surface areas; catalytic activity similar to aerogels	[90]
Grafting of methyl groups on mesoporous TiO_2–SiO_2 xerogels	CH_3Si	TiO_2–SiO_2	Cyclohexene epoxidation with H_2O_2 as oxidant	Hydrophobic catalyst more stable in the presence of water	[88]
Highly porous Al and Nb-containing organosilsesquioxanes	$Si–C_6H_4–Si$, $Si–CH_2C_6H_4CH_2–Si$	Al_2O_3, Nb_2O_5	Gas-phase ethanol dehydration to ethylene	Hydrolysis of Si–C bonds observed at 205 °C	[115]
Methylated aluminosilicates	$CH_3–Si$	Al_2O_3–SiO_2	Gas-phase ethanol dehydration to ethylene	B/L ratio decreased, ethylene selectivity increased	[128]
Aluminosilicates with various organic groups	$C_6H_5CH_2–Si$, $CF_3C_2H_4–Si$, $Si–CH_2–Si$, $Si–C_2H_4–Si$, $Si–CH_2C_6H_4CH_2–Si$	Al_2O_3–SiO_2	Gas-phase ethanol dehydration to ethylene	Ranking of various organic groups in terms of their influence on ethanol conversion and ethylene selectivity developed	[129]
Lewis acidic single site aluminosilicates	$Si(Me)_2–C_3H_6–Si(Me)_2$	$L{\cdot}Al(Si_8O_{20})_3$, L = pyridine, THF	Styrene oxide aminolysis with aniline	Effect on Al site accessibility	[111]
Silicophosphates with P–OH groups on the surface	$Si–C_2H_4–Si$	P_4O_{10}	α-methylstyrene dimerization	Effect on selectivity	[89]
Mixed Ni, Fe phenylphosphonates	$C_6H_5–P$	NiO_6, FeO_6 octahedra	Electrocatalytic water oxidation	Coordination octahedra distorted, activity improved	[98]

[a] This column showing the motives that contain the organic moieties of the hybrid is simply called “organic component” for conciseness, but explicitly shows how the organic group is covalently bound to an inorganic element (e.g. Si, P) of the material matrix.

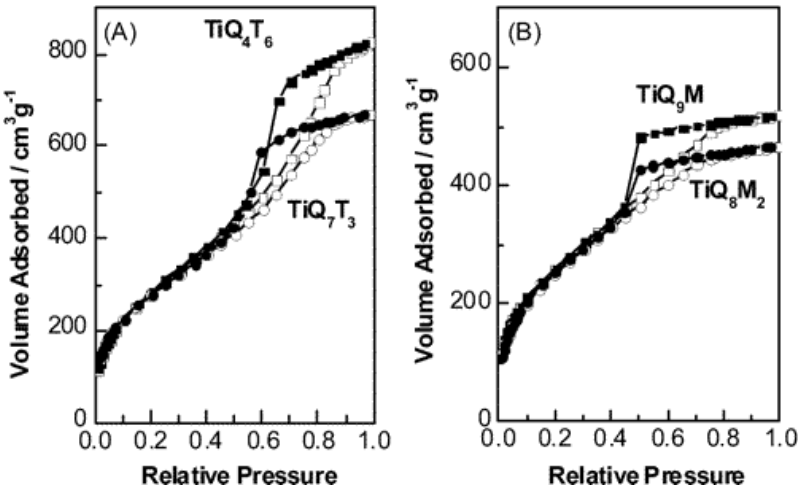

Figure 5: N_2 adsorption-desorption isotherms of hybrid titanosilicates. Sample labels describe molar ratios of particular gel components (Ti stands for $TiCl_4$, Q stands for $SiCl_4$; T stands for CH_3SiCl_3; M stands for Me_3SiCl). Total Si:Ti ratio is always 10. Reprinted with permission from [90]. Copyright (2006) American Chemical Society.

Later on, Smeets *et al.* showed that the post-synthetic hydrophobization of NHSG-made mesoporous TiO_2–SiO_2 epoxidation catalysts could lead to an improvement of the catalyst stability in the presence of an excess of water in the solvent (Figure 6) [88]. More particularly, a purely inorganic TiO_2–SiO_2 xerogel was impregnated with a solution composed of methyltrimethoxysilane dissolved in water-saturated toluene. After 48h, the solid was heated at 90°C for 1 h, washed successively with toluene and pentane, and dried overnight at 120°C under vacuum. The resulting material showed a lower water adsorption (0.52 mg m^{-2}) than the pristine catalyst (1.70 mg m^{-2}) confirming a lower hydrophilicity. The enhanced stability of this catalyst was interpreted in terms of a repelling of water molecules from the active sites. Thus, this hybrid catalyst was more resistant to poisoning and showed higher selectivity values in the epoxidation of cyclohexene with H_2O_2 as oxidant (see Figure 6). However, the one-pot methylation of the xerogel resulted in this case in a lower porosity and lower amounts of accessible active sites. Accordingly, the latter catalysts showed low performance in epoxidation despite the enhanced hydrophobic character (water adsorption of *ca.* 0.4 mg m^{-2}).

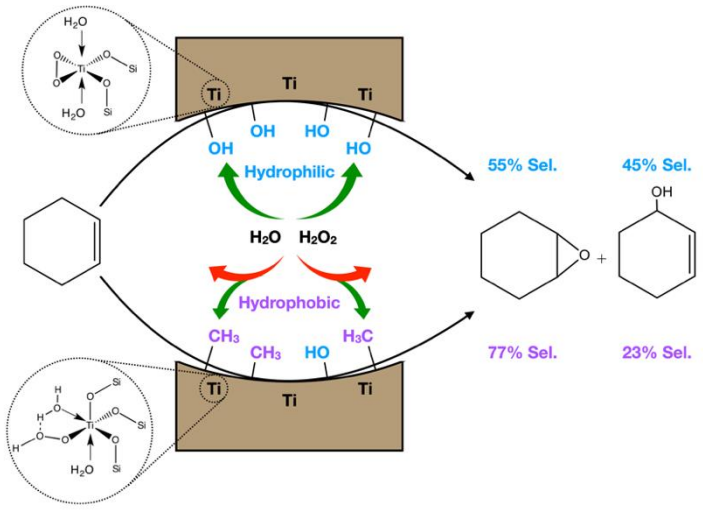

Figure 6: Effect of post-synthetic methylation on the selectivity of TiO_2–SiO_2 catalysts prepared by NHSG used in the epoxidation of cyclohexene with H_2O_2 in the presence of a large excess of water (T = 60°C, 2h reaction time, solvent = acetonitrile/water 75:25 (v/v)) [88].

Gas-phase hydrothermal stability and catalytic ethanol dehydration were studied in porous organosilsesquioxanes prepared in one-pot by alkyl halide and acetamide elimination (surface area up to 880 $m^2\ g^{-1}$ with pore volume of 1.4 $cm^3\ g^{-1}$) [115]. These materials were composed exclusively of $0_{1.5}Si{-}C_6H_4{-}Si0_{1.5}$ units (i.e. silsesquioxanes). While thermal stability of materials containing phenylene bridges has been shown excellent in dry air atmosphere (up to 550 °C, similar to other reports on organosilsequioxanes prepared by hydrolytic sol-gel) [130], the degradation occurred at much lower temperature in the presence of moist air (345 °C). The extent of hybrid materials degradation was reflected mainly in the hydrolysis of Si−C bonds, which was revealed by the evolution of benzene in reaction conditions (GC-MS, Equation (11) and (12)), by a mass loss in TGA, and by the formation of Q sites detected in ^{29}Si MAS NMR spectra (Figure 7). In order to introduce acid sites, these materials were doped with Al or Nb. In this case, the hydrolysis of Si−C bonds, the consequent benzene release, and the transformation of T sites ($CSiO_3$) into Q sites (SiO_4) have been observed at a temperature as low as 205 °C, while the corresponding metal free silsesquioxane was markedly more stable (Figure 7). Noteworthy, the stability of Al- and Nb-doped organosilsequioxanes was markedly improved upon switching from phenylene to xylylene bridges ($0_{1.5}Si{-}CH_2{-}C_6H_4{-}CH_2{-}SiO_{1.5}$); the $Si{-}C_{aliphatic}$ bond proved to be more stable against hydrolysis than $Si{-}C_{aromatic}$ bond. The aluminum doped hybrid material based on xylylene bridges performed gas-phase ethanol dehydration to ethylene with a maximum stability limit of 350 °C without an obvious degradation [115].

$$0_{1.5}Si{-}C_6H_4{-}SiO_{1.5} + H_2O \rightarrow 0_{1.5}Si{-}C_6H_5 + HO{-}SiO_{1.5} \quad (11)$$

$$0_{1.5}Si{-}C_6H_5 + H_2O \rightarrow 0_{1.5}Si{-}OH + C_6H_6 \quad (12)$$

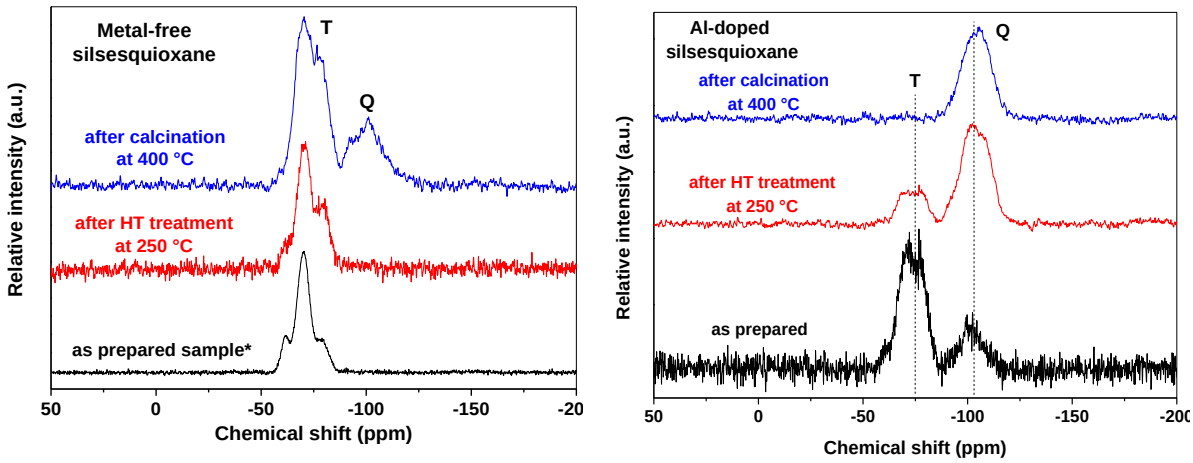

Figure 7: ^{29}Si MAS NMR spectra of metal free silsesquioxane (left) and Al-doped silsesquioxane (right) after various treatments (as prepared – i.e. dried in a flow of dry nitrogen at 250 °C, after hydrothermal treatment at 250 °C, and after calcination at 400 °C). Both materials were composed of $0_{1.5}Si{-}C_6H_4{-}Si0_{1.5}$ units. Observation of Q sites (i.e. SiO_4 units) indicate Si−C bonds rupture (i.e. hybrid material degradation). Reproduced with permission from [115].

In a follow up study, the focus was put on hybrid catalysts having a lower organic groups content (0−10 mol% based on Si) and possessing more stable $Si{-}C_{aliphatic}$ bonds. In this case, the hybrid materials were prepared in one-pot through the introduction of $CH_3{-}Si$ groups and were very similar to purely inorganic benchmark catalyst in terms of porosity (250−290 $m^2\ g^{-1}$), internal structure (IR and MAS NMR spectroscopy), and surface properties (as probed by XPS and ToF-SIMS) [128]. Surprisingly,

hydrophobicity was not strongly affected by the introduction of organic groups; all aluminosilicate catalysts remained highly hydrophilic (as measured by water sorption experiments and by contact angle measurements). Nevertheless, the increasing CH_3−Si groups content caused a marked decrease of Si−OH moieties concentration in hybrid aluminosilicates (as revealed by IR spectroscopy). A lower amount of Si−OH groups available for formation of Brønsted acid pseudo-bridges (Si−O(H)…Al) led to the alteration of the surface acidity: while the total number of acid sites remained similar in hybrid and purely inorganic catalysts, the acid sites were mostly Lewis in nature in hybrid aluminosilicates. On the contrary, the purely inorganic bechnmark catalysts exhibited a higher fraction of Brønsted acid sites. In the gas-phase dehydration of ethanol, the ethylene yields were improved when applying hybrid catalysts mainly owing to the higher ethylene selectivity (Figure 8). The improvement in ethylene selectivity was correlated with the number of Lewis acid sites, which increased upon organic groups introduction at the expense of Brønsted acid sites. Moving further, a dedicated synthetic strategy was proposed, based on the delayed Al addition into the reaction sol. This led to a two-fold increase in the acid site concentration and consequently to a marked ethanol conversion improvement. The high ethylene selectivity was preserved thanks to the presence of the CH_3−Si groups and the associated high proportion of Lewis sites. Such finely tuned methylated aluminosilicate catalyst provided ethylene yields rivalling HZSM-5 [128].

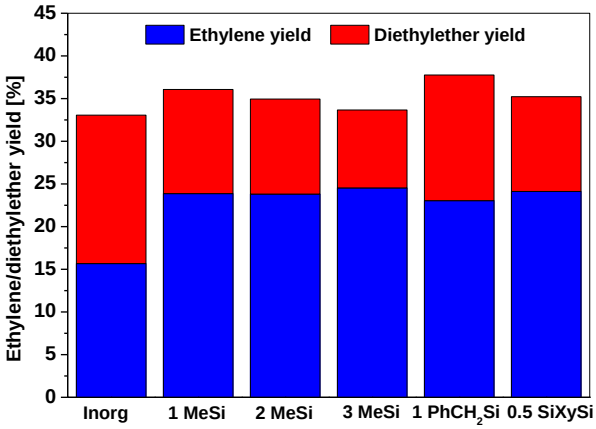

Figure 8: Comparison of ethylene and diethylether yields exhibited by pure inorganic benchmark aluminosilicate catalyst and by hybrid aluminosilicate catalysts with increasing content of CH_3−Si groups (1 MeSi, 2 MeSi, and 3 MeSi) and with varying incorporated organic groups (1 $PhCH_2Si$ and 0.5 SiXySi stand for terminal benzyl- and bridging xylylene groups, respectively). The Si:Al ratio (16) was kept constant within the sample series. Diethylether and ethylene were the only products of gas phase ethanol dehydration and therefore their sum accounts for ethanol conversion. Data taken from Styskalik et al. [128, 129]

The choice of organic groups used to modify aluminosilicate catalysts was broadened in a follow up study [129]. In addition to pendant methyl groups, pendant benzyl and trifluoropropyl groups as well as bridging methylene, ethylene, and xylylene moieties were incorporated into aluminosilicate materials via co-condensation in one pot (alkyl halide elimination) with a nominal content of 6.25 mol% (based on Si). All samples were porous, highly hydrophilic, and Al was homogeneously distributed within the bulk of the materials with no obvious alumina cluster formation (^{27}Al MAS NMR). Nevertheless, the samples containing aromatic groups (both terminal benzyl and bridging xylylene) exhibited slightly better Al-Si mixing in the top surface layer (ToF-SIMS) and higher total acid site numbers (IR-pyridine). These two samples exhibited better catalytic performance than purely inorganic benchmark: the ethylene yields were improved mainly due to the higher ethylene selectivity (Figure 8, samples 1 $PhCH_2Si$ and 0.5 SiXySi). This was again connected to a higher Lewis acid site

numbers in hybrid aluminosilicates. The catalysts modified with methylene and ethylene bridging units, however, performed slightly poorer. The influence of sample hydrophilicity/hydrophobicity on catalytic performance seemed improbable as no correlation was observed between the two parameters. Instead, the lower performance could be correlated with a lower number of surface acid sites. All in all, this study estimated a "ranking" in a variety of organic groups in terms of their effect on gas-phase ethanol dehydration to ethylene; ethylene yield was decreasing in this order: bridging xylylene ≈ pendant methyl > pendant benzyl > bridging methylene ≈ inorganic benchmark (no organic groups) > bridging ethylene [129].

The choice of organic bridges decisively influences active site accessibility, as it was shown in a study working with Lewis acid single site aluminosilicate catalysts [111]. Well-defined catalytic sites based on Al atoms connected via three Al−O−Si bridges and with the fourth coordination site occupied by neutral base ligand (THF or pyridine) were kept isolated thanks to their direct bonding to bulky Si_8O_{20} siloxane building blocks (Figure 9, Dose 1). These "silicate cubes" were further cross-linked by different chlorosilanes in order to create porous materials (Figure 9, Dose 2): dichlorodimethylsilane, 1,2-bis(chlorodimethylsilyl)ethane, and 1,3-bis(chlorodimethylsilyl)propane. All synthetic steps were performed in strictly anhydrous conditions. The accessibility of catalytic sites was studied by a simple "titration" experiment based on ligand exchange on Al atoms (THF for pyridine, Equation (13)) followed by ^{1}H NMR spectroscopy. While a weaker base ligand coordinated to Al site (Figure 9) could be completely exchanged for a stronger base in materials cross-linked with flexible $OSi(Me)_2{-}C_3H_6{-}Si(Me)_2O$ and $OSi(Me)_2{-}C_2H_4{-}Si(Me)_2O$ bridges, the same ligand exchange reaction occurred only partially in hybrid aluminosilicates cross-linked with the shorter Me_2SiO_2 units. This showed that not all Al sites were accessible when a small and rigid cross-linking unit was applied. These observations correlated well with catalytic activity in styrene oxide aminolysis with aniline: the better the Al site accessibility, the higher the catalytic activity. All catalysts exhibited a selectivity close to 100 % to the expected Markovnikov product of the catalytic reaction [111].

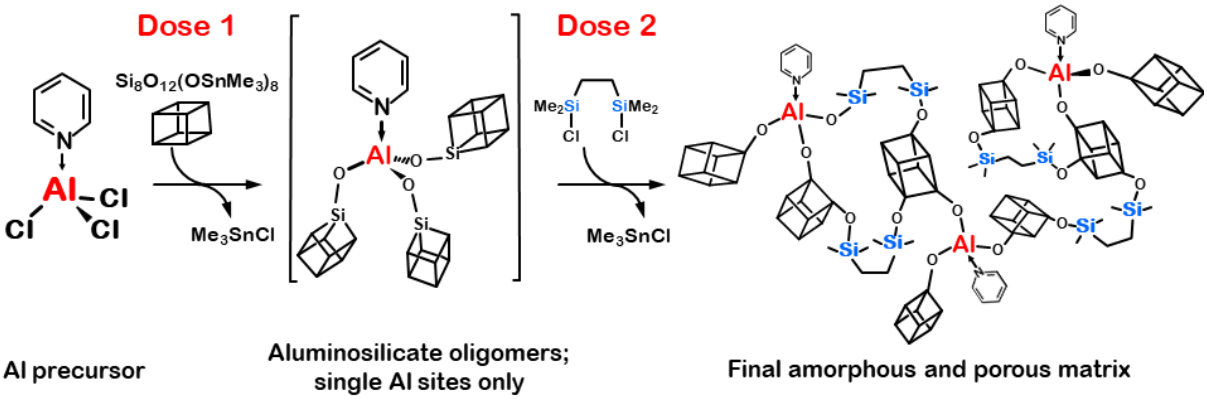

Figure 9: Reaction procedure based on sequential dosing providing Lewis acid single site aluminosilicate catalysts with targeted coordination number and connectivity to siloxane matrix. Adapted with permission from [111].

$$(\equiv Si{-}O)_3Al{\cdot}THF + 2\ Py \rightarrow (\equiv Si{-}O)_3Al{\cdot}Py + THF + Py \qquad (13)$$

Hybrid silicophosphate materials containing Si−C or P−C linkages were prepared by ester elimination reaction [101]. The introduction of organic groups bound to Si atoms had a marked effect on the structure of these materials: octahedrally coordinated Si atoms were not observed in the hybrid

materials (Figure 10, left) in contrary to purely inorganic samples. At the same time, the porosity changed significantly: while inorganic materials were microporous, the hybrids containing Si−C bonds were mostly mesoporous. Hybrid silicophosphate with $Si-C_2H_4-Si$ moieties was chosen for further surface grafting and catalytic performance studies and compared to the inorganic silicophosphate benchmark. The surface of both hybrid and inorganic silicophosphate materials was grafted and/or reacted with a number of chemicals including hexamethyldisiloxane, benzyltrichlorosilane, $SiCl_4$, methanol, water, $AlCl_3$, $AlMe_3$, $Al(NMe_2)_3$, and $POCl_3$ [89]. The controlled hydrolysis reactions created acidic P−OH groups on the surface, which were highly active in α-methylstyrene dimerization (catalyzed by Brønsted acids, Figure 10, right). Interestingly, the mesoporous hybrid catalysts exhibited the highest selectivity to a methylstyrene dimer with terminal double bond (II), while the purely inorganic microporous material provided dimers with bridging double bond (III, cis and trans) with the highest selectivity (dimer (I) selectivity was low in both cases). The α-methylstyrene conversions for both catalysts were comparable [89].

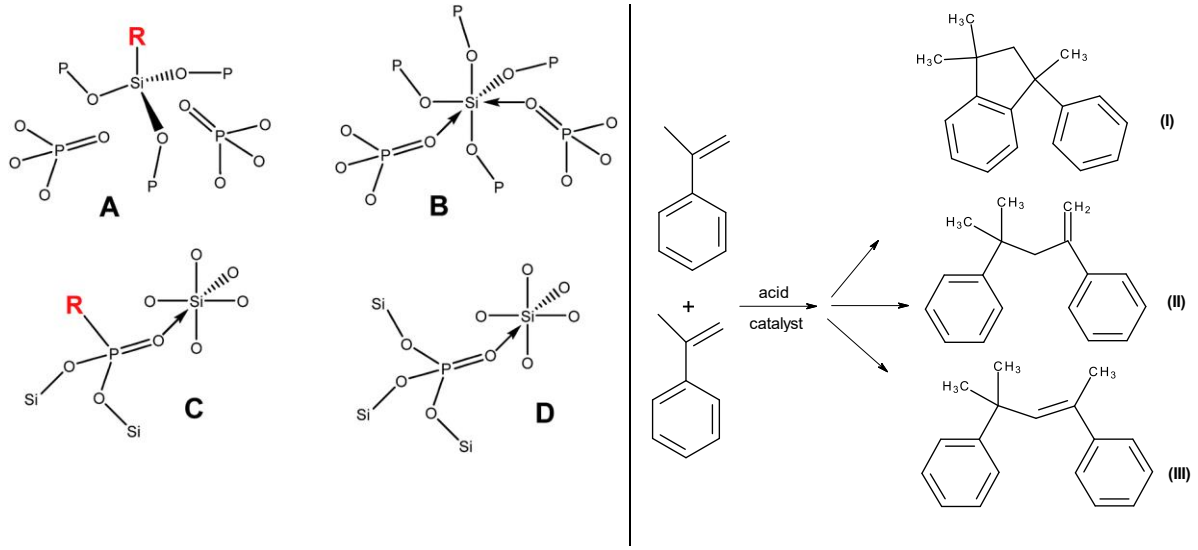

Figure 10: Left: Si coordination environments observed in hybrid silicophosphates containing Si−C bonds (A), pure inorganic silicophosphates (B and D), and hybrid silicophosphonates containing P−C bonds (C) [101] - Published by The Royal Society of Chemistry. Right: α-methylstyrene dimers possibly formed by acid-catalyzed reaction [89] - Published by The Royal Society of Chemistry (RSC) on behalf of the Centre National de la Recherche Scientifique (CNRS) and the RSC.

The synthesis of hybrid materials containing P−C bonds (i.e. metal phosphonates) has been achieved by several NHSG pathways [61, 93, 95, 97-99, 101]. However, only Zhang et al. used such hybrid materials as heterogeneous catalysts, namely in electrocatalytic water oxidation [98, 99]. Mixed Ni, Fe phenylphosphonates were prepared by the benzyl alcohol route in the whole range of possible Ni and Fe contents (0−100 wt%). The most active catalyst, exhibiting the lowest overpotential, was identified as a mixed Ni, Fe phenylphosphonate with a Fe content of 16 wt% (Figure 11a). These metal phosphonate materials exhibited layered structures, as confirmed by XRD analyses (Figure 11b), with Ni and Fe occupying distorted octahedral positions. The deviation from ideal octahedral symmetry was confirmed by detailed XANES (pre-edge) and EXAFS studies and deemed crucial for the observed improved behavior in electrocatalytic water oxidation. It has been shown that the phenylphosphonates leached out of the materials during the electrocatalytic reaction. However, the resulting Ni,Fe hydroxides kept the distortion of coordination polyhedrons thus providing in a stable catalytic performance. The overpotential in NHSG prepared mixed Ni, Fe phenylphoshonate with

16 wt% Fe was markedly lower than in metal hydroxides prepared by conventional routes, where the distortion of coordination polyhedrons has not been observed (Figure 11c). This led to an improved electrocatalytic activity in comparison to conventional benchmarks [98].

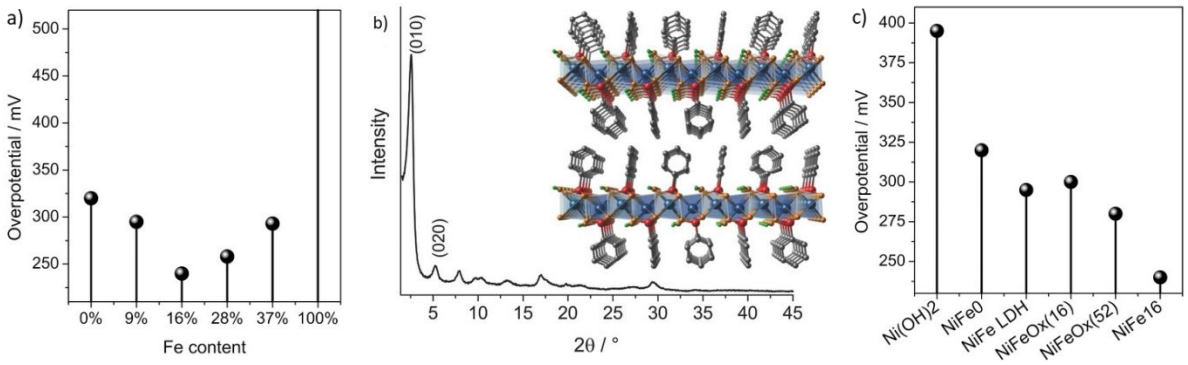

Figure 11: a) Comparison of overpotentials of mixed Fe,Ni phenylphosphonate catalysts prepared by NHSG with varying Fe content in electrocatalytic water oxidation (the lower the overpotential, the more active the catalyst). b) XRD diffractogram of prepared sample with 16 % Fe content and suggested layered metal phenylphosphonate structure, FeO_6 and NiO_6 octahedra distorted. c) Comparison of overpotentials of mixed Fe,Ni phenylphosphonate catalyst with 16 % Fe content with benchmark catalysts in electrocatalytic water oxidation. Adapted with permission from [98].

4. Conclusions

Hybrid materials have a bright forecast in the field of heterogeneous catalysis. Hybrid catalysts often present decisive advantages compared to their purely inorganic analogs, including enhanced activity and/or selectivity, and facilited mass tranfer in the solid. In terms of stability, hybrid catalysts can reach better performance against for example liquid phase leaching, or adsorption of poisons. This being said, the window of conditions that can be used for preparation and operation may be restricted in the view of the limited thermal stability of the organic moieties. Stability issues with hybrid catalysts are often overlooked in the literature and we argue that further efforts should be devoted to these aspects.

Through the examples covered in this review, we show that non-hydrolytic sol-gel routes are emerging as a highly potent toolbox for the preparation of Class I and Class II hybrid catalysts. Among others, NHSG allows obtaining a broad variety of compositions *via* a limited number of steps while effectively controlling key properties such as the catalyst texture and the distribution of the inorganic and organic moieties in the solid. This is obtained firstly thanks to the use of non aqueous conditions in which the kinetics of solvolysis and polycondensation reactions are easily controlled. Secondly, the use of volatile solvents which have a much lower surface tension as compared to water facilitates the drying step and gives access to highly open textures. Working in non aqueous conditons is also crucial for the heterogeneization of homogeneous catalysts. For example, some organometallics and metal complexes used as catalysts may be inactivated when encapsulated in inorganic materials via hydrolytic routes, whereas they retain their activity in non aqueous conditions. Starting from hybrid precursors, the incoproation of a wide series of organic moieties in oxide and mixed oxide materials was shown to be straightforward. Based on these unique features, we anticipate that NHSG routes will continue to allow catalysis scientists exploring pristine chemical spaces for the prepararion of advances hybrid catalysts, thereby also expanding the range of potential applications.

References

[1] JN Armor (2011) Catalysis Today 163: 3. Doi:10.1016/j.cattod.2009.11.019
[2] I Fechete, Y Wang, JC Védrine (2012) Catalysis Today 189: 2. Doi:10.1016/j.cattod.2012.04.003
[3] A Primo, H Garcia (2014) Chemical Society Reviews 43: 7548. Doi:10.1039/c3cs60394f
[4] XS Zhao, GQ Lu, GJ Millar (1996) Industrial & Engineering Chemistry Research 35: 2075. Doi:10.1021/ie950702a
[5] R Gérardy, DP Debecker, J Estager, P Luis, J-CM Monbaliu (2020) Chemical Reviews 120: 7219. Doi:10.1021/acs.chemrev.9b00846
[6] H Kobayashi, H Ohta, A Fukuoka (2012) Catalysis Science & Technology 2: 869. Doi:10.1039/C2CY00500J
[7] C Sanchez, P Belleville, M Popall, L Nicole (2011) Chemical Society Reviews 40: 696. Doi:10.1039/c0cs00136h
[8] B Arkles (2011) MRS Bulletin 26: 402. Doi:10.1557/mrs2001.94
[9] C Sanchez, F Ribot (1994) New Journal of Chemistry 18: 1007.
[10] A Vivian, L Soumoy, L Fusaro, SL Fiorilli, DP Debecker, C Aprile (2020) Green Chemistry. Doi:10.1039/D0GC02562C
[11] AH Chughtai, N Ahmad, HA Younus, A Laypkov, F Verpoort (2015) Chem Soc Rev 44: 6804. Doi:10.1039/c4cs00395k
[12] J Lee, OK Farha, J Roberts, KA Scheidt, ST Nguyen, JT Hupp (2009) Chem Soc Rev 38: 1450. Doi:10.1039/b807080f
[13] P Van der Voort, D Esquivel, E De Canck, F Goethals, I Van Driessche, FJ Romero-Salguero (2013) Chem Soc Rev 42: 3913. Doi:10.1039/c2cs35222b
[14] S Rostamnia, E Doustkhah (2014) RSC Advances 4: 28238. Doi:10.1039/c4ra03773a
[15] L van den Biggelaar, P Soumillion, DP Debecker (2019) RSC Advances 9: 18538. Doi:10.1039/c9ra02433f
[16] RA Sheldon, S van Pelt (2013) Chemical Society Reviews 42: 6223. Doi:10.1039/c3cs60075k
[17] V Smeets, W Baaziz, O Ersen, et al. (2020) Chemical Science 11: 954. Doi:10.1039/c9sc04615a
[18] S Dutta, N Kumari, S Dubbu, et al. (2020) Angewandte Chemie International Edition 59: 3416. Doi:10.1002/anie.201916578
[19] DP Debecker, V Smeets, M Van der Verren, H Meerssman Arango, M Kinnaer, F Devred (2020) Current Opinion in Green and Sustainable Chemistry: 100437. Doi:10.1016/j.cogsc.2020.100437
[20] MH Valkenberg, WF Hölderich (2002) Catalysis Reviews 44: 321. Doi:10.1081/cr-120003497
[21] M Polakovic, J Svitel, M Bucko, et al. (2017) Biotechnology Letters 39: 667. Doi:10.1007/s10529-017-2300-y
[22] DP Debecker (2018) The Chemical Record 18: 662. Doi:10.1002/tcr.201700068
[23] DA Ward, EI Ko (1995) Industrial & Engineering Chemistry Research 34: 421. Doi:10.1021/ie00041a001
[24] LL Hench, JK West (1990) Chemical Reviews 90: 33. Doi:10.1021/cr00099a003
[25] C Sanchez, L Rozes, F Ribot, et al. (2010) Comptes Rendus Chimie 13: 3. Doi:10.1016/j.crci.2009.06.001
[26] W Gerrard, PF Griffey (1959) Chemistry & Industry: 55.
[27] DA Lindquist, SM Poindexter, SS Rooke, et al. (1994) Proceedings Arkansas Academy of Science 48: 100.
[28] J Goubeau, KO Christe, W Teske, W Wilborn (1963) Zeitschrift fur anorganische und allgemeine Chemie 325: 26. Doi:10.1002/zaac.19633250106
[29] M Andrianainarivelo, R Corriu, D Leclercq, PH Mutin, A Vioux (1996) Journal of Materials Chemistry 6: 1665. Doi:10.1039/jm9960601665
[30] DP Debecker, V Hulea, PH Mutin (2013) Applied Catalysis A-General 451: 192. Doi:10.1016/j.apcata.2012.11.002
[31] PH Mutin, A Vioux (2009) Chemistry of Materials 21: 582. Doi:10.1021/cm802348c
[32] A Styskalik, D Skoda, CE Barnes, J Pinkas (2017) Catalysts 7: 168. Doi:10.3390/catal7060168

[33] DP Debecker, PH Mutin (2012) Chemical Society Reviews 41: 3624. Doi:10.1039/c2cs15330k
[34] C Le Roux, H Yang, S Wenzel, S Grigoras, MA Brook (1998) Organometallics 17: 556. Doi:10.1021/om970953e
[35] AR Bassindale, IA MacKinnon, MG Maesano, PG Taylor (2003) Chemical Communications: 1382. Doi:10.1039/b302556j
[36] J Podhorsky, J Chyba, J Pinkas, Z Moravec (2019) Journal of Sol-Gel Science and Technology 91: 385. Doi:10.1007/s10971-019-04953-0
[37] I Djerdj, D Arcon, Z Jaglicic, M Niederberger (2008) Journal of Solid State Chemistry 181: 1571. Doi:10.1016/j.jssc.2008.04.016
[38] G Garnweitner, M Niederberger (2006) Journal of the American Ceramic Society 89: 1801. Doi:10.1111/j.1551-2916.2006.01005.x
[39] M Niederberger (2007) Acc Chem Res 40: 793. Doi:10.1021/ar600035e
[40] M Niederberger, G Garnweitner (2006) Chemistry - A European Journal 12: 7282. Doi:10.1002/chem.200600313
[41] M Niederberger, G Garnweitner, J Buha, J Polleux, J Ba, N Pinna (2006) Journal of Sol-Gel Science and Technology 40: 259. Doi:10.1007/s10971-006-6668-8
[42] N Pinna, G Garnweitner, M Antonietti, M Niederberger (2005) Journal of the American Chemical Society 127: 5608. Doi:10.1021/ja042323r
[43] I Bilecka, M Niederberger (2010) Electrochimica Acta 55: 7717. Doi:10.1016/j.electacta.2009.12.066
[44] DC Bradley, IM Thomas (1959) Journal of the Chemical Society (Resumed): 3404. Doi:10.1039/jr9590003404
[45] J Caruso, MJ Hampden-Smith (1997) Journal of Sol-Gel Science and Technology 8: 35. Doi:10.1023/a:1026466130856
[46] J Caruso, MJ Hampden-Smith, EN Duesler (1995) Journal of the Chemical Society, Chemical Communications 2: 1041. Doi:10.1039/c39950001041
[47] M Jansen, E Guenther (1995) Chemistry of Materials 7: 2110. Doi:10.1021/cm00059a019
[48] M Iwasaki, A Yasumori, S Shibata, M Yamane (1994) Journal of Sol-Gel Science and Technology 2: 387. Doi:10.1007/bf00486276
[49] A Styskalik, D Skoda, Z Moravec, JG Abbott, CE Barnes, J Pinkas (2014) Microporous and Mesoporous Materials 197: 204. Doi:10.1016/j.micromeso.2014.06.019
[50] D Skoda, A Styskalik, Z Moravec, et al. (2016) RSC Advances 6: 24273. Doi:10.1039/c5ra24563j
[51] D Skoda, A Styskalik, Z Moravec, P Bezdicka, CE Barnes, J Pinkas (2015) Journal of Sol-Gel Science and Technology 74: 810. Doi:10.1007/s10971-015-3666-8
[52] D Skoda, A Styskalik, Z Moravec, et al. (2016) RSC Advances 6: 68739. Doi:10.1039/c6ra16556g
[53] D Skoda, A Styskalik, Z Moravec, P Bezdicka, J Pinkas (2015) Journal of Materials Science 50: 3371. Doi:10.1007/s10853-015-8888-1
[54] A Styskalik, D Skoda, J Pinkas, S Mathur (2012) Journal of Sol-Gel Science and Technology 63: 463. Doi:10.1007/s10971-012-2808-5
[55] A Styskalik, V Vykoukal, L Fusaro, C Aprile, DP Debecker (2020) Applied Catalysis B: Environmental 271: 118926. Doi:10.1016/j.apcatb.2020.118926
[56] MA Brook, JB Grande, F Ganachaud (2010) Springer Berlin Heidelberg,
[57] DB Thompson, MA Brook (2008) Journal of American Chemical Society 130: 32. Doi:10.1021/ja0778491
[58] J Chojnowski, S Rubinsztajn, JA Cella, et al. (2005) Organometallics 24: 6077. Doi:10.1021/om050563p
[59] J Kurjata, W Fortuniak, S Rubinsztajn, J Chojnowski (2009) European Polymer Journal 45: 3372. Doi:10.1016/j.eurpolymj.2009.10.004
[60] S Rubinsztajn (2014) Journal of Inorganic and Organometallic Polymers and Materials 24: 1092. Doi:10.1007/s10904-014-0094-0
[61] P Machac, JG Alauzun, A Styskalik, DP Debecker, PH Mutin, J Pinkas (2021) Microporous and Mesoporous Materials 311: 110682. Doi:10.1016/j.micromeso.2020.110682

[62] J Pinkas, H Wessel, Y Yang, et al. (1998) Inorganic Chemistry 37: 2450. Doi:10.1021/ic9713036
[63] JW Kriesel, MS Sander, TD Tilley (2001) Chemistry of Materials 13: 3554. Doi:10.1021/cm010068t
[64] DC Bradley, BN Charkravarti, AK Chatterjee, W Wardlaw, A Whitley (1958) Journal of the Chemical Society (Resumed): 99. Doi:10.1039/jr9580000099
[65] R Pazik, R Tekoriute, S Hakansson, et al. (2009) Chemistry - A European Journal 15: 6820. Doi:10.1002/chem.200900836
[66] AA Bernardes, GL Scheffler, C Radtke, D Pozebon, JHZ dos Santos, ZN da Rocha (2020) Colloids and Surfaces A: Physicochemical and Engineering Aspects 584: 124020. Doi:10.1016/j.colsurfa.2019.124020
[67] LB Capeletti, MDM Alves, MB Cardoso, JHZ dos Santos (2018) Applied Catalysis A: General 560: 225. Doi:10.1016/j.apcata.2018.03.013
[68] AG Fisch, NSM Cardozo, AR Secchi, et al. (2009) Applied Catalysis A: General 354: 88. Doi:10.1016/j.apcata.2008.11.013
[69] AG Fisch, NSM Cardozo, AR Secchi, et al. (2009) Applied Catalysis A: General 370: 114. Doi:10.1016/j.apcata.2009.09.032
[70] AG Fisch, NSM Cardozo, AR Secchi, FC Stedile, NPd Silveira, JHZ dos Santos (2008) Journal of Non-Crystalline Solids 354: 3973. Doi:10.1016/j.jnoncrysol.2008.05.018
[71] MA Ullmann, JHZ dos Santos (2020) Journal of Catalysis 385: 30. Doi:10.1016/j.jcat.2020.03.001
[72] JMA Caiut, S Nakagaki, OJ De Lima, et al. (2003) Journal of Sol-Gel Science and Technology 28: 57. Doi:10.1023/a:1025685019670
[73] OJ de Lima, DP de Aguirre, DC de Oliveira, et al. (2001) Journal of Materials Chemistry 11: 2476. Doi:10.1039/b100897h
[74] TCO Mac Leod, DFC Guedes, MR Lelo, et al. (2006) Journal of Molecular Catalysis A: Chemical 259: 319. Doi:10.1016/j.molcata.2006.07.022
[75] M Saltarelli, EH de Faria, KJ Ciuffi, et al. (2019) Molecular Catalysis 462: 114. Doi:10.1016/j.mcat.2018.09.014
[76] A Fisch, CF Petry, D Pozebon, et al. (2006) Macromolecular Symposia 245: 77. Doi:10.1002/masy.200651311
[77] A Styskalik, D Skoda, Z Moravec, P Roupcova, CE Barnes, J Pinkas (2015) RSC Advances 5: 73670. Doi:10.1039/c5ra10982e
[78] C Warwar Damouny, N Hayek, C Khoury, OM Gazit (2019) ACS Applied Energy Materials 2: 6505. Doi:10.1021/acsaem.9b01086
[79] C Warwar Damouny, C Khoury, OM Gazit (2019) Journal of the American Ceramic Society 102: 456. Doi:10.1111/jace.15904
[80] F Bottger-Hiller, R Lungwitz, A Seifert, et al. (2009) Angewandte Chemie International Edition 48: 8878. Doi:10.1002/anie.200903636
[81] A Mehner, T Rüffer, H Lang, A Pohlers, W Hoyer, S Spange (2008) Advanced Materials 20: 4113. Doi:10.1002/adma.200801376
[82] S Spange, P Kempe, A Seifert, et al. (2009) Angewandte Chemie International Edition 48: 8254. Doi:10.1002/anie.200901113
[83] C Leonhardt, S Brumm, A Seifert, et al. (2013) ChemPlusChem 78: 1400. Doi:10.1002/cplu.201200242
[84] C Schliebe, T Gemming, J Noll, et al. (2015) ChemPlusChem 80: 559. Doi:10.1002/cplu.201402338
[85] J Weißhuhn, A Seifert, V Dzhagan, et al. (2018) Macromolecular Chemistry and Physics 219: 1700487. Doi:10.1002/macp.201700487
[86] C Schliebe, J Noll, S Scharf, et al. (2018) Colloid and Polymer Science 296: 413. Doi:10.1007/s00396-017-4254-y
[87] I Olliges-Stadler, MD Rossell, M Niederberger (2010) Small 6: 960. Doi:10.1002/smll.200902289
[88] V Smeets, L Ben Mustapha, J Schnee, EM Gaigneaux, DP Debecker (2018) Molecular Catalysis 452: 123. Doi:10.1016/j.mcat.2018.04.011

[89] A Styskalik, D Skoda, Z Moravec, CE Barnes, J Pinkas (2016) New Journal of Chemistry 40: 3705. Doi:10.1039/c5nj02928g
[90] O Lorret, V Lafond, PH Mutin, A Vioux (2006) Chemistry of Materials 18: 4707. Doi:10.1021/cm061478q
[91] L Bourget, PH Mutin, A Vioux, JM Frances (1998) Journal of Polymer Science Part a-Polymer Chemistry 36: 2415. Doi:10.1002/(SICI)1099-0518(19980930)36:13<2415::AID-POLA28>3.0.CO;2-C
[92] L Crouzet, D Leclercq, PH Mutin, A Vioux (2003) Journal of Sol-Gel Science and Technology 26: 335. Doi:10.1023/a:1020792208751
[93] RJP Corriu, D Leclercq, PH Mutin, L Sarlin, A Vioux (1998) Journal of Materials Chemistry 8: 1827. Doi:10.1039/a803755h
[94] G Guerrero, JG Alauzun, M Granier, D Laurencin, PH Mutin (2013) Dalton Transactions 42: 12569. Doi:10.1039/c3dt51193f
[95] G Guerrero, PH Mutin, A Vioux (2001) Journal of Materials Chemistry 11: 3161. Doi:10.1039/b104411g
[96] PH Mutin, G Guerrero, JG Alauzun, PE Bataillon, FM Cedex (2015) J. Ceram. Soc. JAPAN 123: 709. Doi:10.2109/jcersj2.123.709
[97] YH Wang, JG Alauzun, PH Mutin (2020) Chemistry of Materials 32: 2910. Doi:10.1021/acs.chemmater.9b05095
[98] R Zhang, PA Russo, AG Buzanich, T Jeon, N Pinna (2017) Advanced Functional Materials 27: 1703158. Doi:10.1002/adfm.201703158
[99] R Zhang, PA Russo, M Feist, P Amsalem, N Koch, N Pinna (2017) ACS Appl Mater Interfaces 9: 14013. Doi:10.1021/acsami.7b01178
[100] N Pinna (2007) J. Mater. Chem. 17: 2769. Doi:10.1039/b702854g
[101] A Styskalik, D Skoda, Z Moravec, M Babiak, CE Barnes, J Pinkas (2015) Journal of Materials Chemistry A 3: 7477. Doi:10.1039/c4ta06823h
[102] M Kejik, Z Moravec, CE Barnes, J Pinkas (2017) Microporous and Mesoporous Materials 240: 205. Doi:10.1016/j.micromeso.2016.11.012
[103] R Wakabayashi, K Kawahara, K Kuroda (2010) Angewandte Chemie International Edition 49: 5273. Doi:10.1002/anie.201001640
[104] R Wakabayashi, M Tamai, K Kawahara, et al. (2012) Journal of Organometallic Chemistry 716: 26. Doi:10.1016/j.jorganchem.2012.05.033
[105] S Saito, N Yamasue, H Wada, A Shimojima, K Kuroda (2016) Chemistry 22: 13857. Doi:10.1002/chem.201601906
[106] M Yoshikawa, Y Tamura, R Wakabayashi, M Tamai, A Shimojima, K Kuroda (2017) Angewandte Chemie International Edition 56: 13990. Doi:10.1002/anie.201705942
[107] J Pinkas, D Chakraborty, Y Yang, R Murugavel, M Noltemeyer, HW Roesky (1999) Organometallics 18: 523. Doi:10.1021/om9806702
[108] CE Barnes, K Sharp, AA Albert, ME Peretich, P Fulvio (2015) Journal of Nanoscience Letters 5: 1.
[109] NN Ghosh, JC Clark, GT Eldridge, CE Barnes (2004) Chemical Communications: 856. Doi:10.1039/b316184f
[110] MY Lee, JA Jiao, R Mayes, E Hagaman, CE Barnes (2011) Catalysis Today 160: 153. Doi:10.1016/j.cattod.2010.06.029
[111] A Styskalik, JG Abbott, MC Orick, DP Debecker, CE Barnes (2019) Catalysis Today 334: 131. Doi:10.1016/j.cattod.2018.11.079
[112] K Kawahara, Y Hagiwara, K Kuroda (2011) Chemistry - A European Journal 17: 13188. Doi:10.1002/chem.201102205
[113] JC Clark, CE Barnes (2007) Chemistry of Materials 19: 3212. Doi:10.1021/cm070038b
[114] M Yoshikawa, H Shiba, H Wada, A Shimojima, K Kuroda (2018) Bulletin of the Chemical Society of Japan 91: 747. Doi:10.1246/bcsj.20170410
[115] A Styskalik, I Kordoghli, C Poleunis, et al. (2020) Microporous and Mesoporous Materials 297: 110028. Doi:10.1016/j.micromeso.2020.110028

[116] S Maksasithorn, P Praserthdam, K Suriye, M Devillers, DP Debecker (2014) Applied Catalysis A: General 488: 200. Doi:10.1016/j.apcata.2014.09.030
[117] K Bouchmella, M Stoyanova, U Rodemerck, DP Debecker, P Hubert Mutin (2015) Catalysis Communications 58: 183. Doi:10.1016/j.catcom.2014.09.024
[118] YP Du, F Heroguel, JS Luterbacher (2018) Small 14: e1801733. Doi:10.1002/smll.201801733
[119] V Lafond, PH Mutin, A Vioux (2002) Journal of Molecular Catalysis A: Chemical 182-183: 81. Doi:10.1016/s1381-1169(01)00487-3
[120] AM Cojocariu, PH Mutin, E Dumitriu, F Fajula, A Vioux, V Hulea (2008) Chemical Communications: 5357. Doi:10.1039/b811668g
[121] DD Dochain, A Stýskalík, DP Debecker (2019) Catalysts 9: 920. Doi:10.3390/catal9110920
[122] DP Debecker, K Bouchmella, R Delaigle, et al. (2010) Applied Catalysis B: Environmental 94: 38. Doi:10.1016/j.apcatb.2009.10.018
[123] C Petitto, HP Mutin, G Delahay (2013) Applied Catalysis B: Environmental 134-135: 258. Doi:10.1016/j.apcatb.2013.01.018
[124] C Petitto, PH Mutin, G Delahay (2013) Topics in Catalysis 56: 34. Doi:10.1007/s11244-013-9925-4
[125] AG Fisch, N da Silveira, NSM Cardozo, AR Secchi, JHZ dos Santos, JBP Soares (2013) Journal of Molecular Catalysis A: Chemical 366: 74. Doi:10.1016/j.molcata.2012.08.028
[126] MA Ullmann, JHZ dos Santos (2019) Journal of Catalysis 378: 226. Doi:10.1016/j.jcat.2019.08.040
[127] JHZ dos Santos (1999) Journal of Molecular Catalysis A: Chemical 139: 199. Doi:10.1016/s1381-1169(98)00173-3
[128] A Styskalik, I Kordoghli, C Poleunis, et al. (2020) Journal of Materials Chemistry A 8: 23526. Doi:10.1039/d0ta07016e
[129] D Debecker, F Devred, L Fusaro, et al. (2020). Doi:10.26434/chemrxiv.13377212
[130] D Esquivel, C Jimenez-Sanchidrian, FJ Romero-Salguero (2011) Journal of Materials Chemistry 21: 724. Doi:10.1039/c0jm02980g